scientific reports

Check for updates

OPEN

Histomorphometric analysis of anterior cruciate ligament bundles and anatomical insights into injury mechanisms

In-Seung Yeo[1,2], Ju-Eun Hong[3] & Hun-Mu Yang[2,4]✉

The anterior cruciate ligament consists of two bundles, the anteromedial and posterolateral bundles, which are frequently associated with meniscal dysfunction. Despite previous studies investigating the relationship between biomechanical instability and injury, a comprehensive histological analysis of the anatomical aspects contributing to injury and degenerative changes and the structural connectivity between the anterior cruciate ligament and the meniscus is lacking. Masson's trichrome, pentachrome, Safranin-O, and modified Verhoeff-Van Gieson histological stains and microcomputed tomography were used in this analysis. The anteromedial bundle of the anterior cruciate ligament is tightly connected to the medial meniscus via articular cartilage, whereas the posterolateral bundle is loosely connected to the transition zone of the lateral meniscus via connective tissue. Due to the differences in the structural connectivity between the meniscus and each anterior cruciate ligament bundle, the degree of deformation of the space between the two bundles varies significantly with knee flexion angle. Furthermore, the two bundles exhibit histological differences in the ratio of elastic fibers to collagen at regions. Specifically, the ratios of the upper and lower parts were 11.36 ± 0.90% and 4.87 ± 0.34%, respectively, for the anteromedial bundle, and 10.33 ± 0.37% and 5.32 ± 0.78%, respectively, for the posterolateral bundle.

Keywords Anterior cruciate ligament, Medial meniscus, Lateral meniscus, Anatomy, Articular cartilage

Abbreviations

ACL	Anterior cruciate ligament
Ac	Articular cartilage
AM	Anterior cruciate ligament-anteromedial bundle
alm	Anterior horn of lateral meniscus
aMM	Anterior horn of medial meniscus
Ct	Connective tissue
GAG	Glycosaminoglycan
ICE	Intercondylar eminence
LM	Lateral meniscus
MM	Medial meniscus
MT	Masson's trichrome staining
PC	Pentachrome staining
PL	Anterior cruciate ligament-posterolateral bundle
Saf-O	Safranin-O staining
VG	Modified Verhoeff-Van Gieson staining

The knee joint is a complex structure that provides both stability and mobility to the body, which are achieved through the interactions between the anterior cruciate ligament (ACL) and the meniscus[1]. Acting as shock

[1]Department of Anatomy, College of Medicine, The Soonchunhyang University of Korea, Dongnam-Gu, Cheonan-si 31151, Chungcheongnam-do, Republic of Korea. [2]Translational Research Unit for Anatomy and Analgesia, Seoul, Republic of Korea. [3]Department of Biomedical Laboratory Science, College of Software and Digital Healthcare convergence, Yonsei University MIRAE Campus, Wonju, Republic of Korea. [4]Department of Anatomy, Yonsei University College of Medicine, 50-1 Yonsei-ro, Seodaemun-gu, Seoul 03722, Republic of Korea. ✉email: yanghm@yuhs.ac

absorbers and weight distributors, the menisci play a crucial role in enhancing knee stability alongside the ACL. The ACL comprises two bundles: the anteromedial (AM) bundle and the posterolateral (PL) bundle[2]. Tensile forces exerted on the ACL are influenced by the angle of the knee, resulting in intricate mechanical interactions with the corresponding meniscus, particularly during rotational movements with flexion. Injuries that affect these structures may lead to them rupturing simultaneously[3–5]. Researchers have investigated the roles played by the ACL bundles in determining mechanical tension on the knee[6–8] and the prevalence of recurrent injuries due to reciprocal failure[9]. Recent anatomical and biomechanical studies have explored the macroscopic attachments between the ACL and meniscus and their biomechanical interactions[10,11]. While research on the interconnectivity of the ACL, transverse ligament, and meniscus has contributed to understanding the cause of injury[12,13], conflicting results have been documented[14,15]. Unfortunately, there is still insufficient anatomical information available on the macroscopic properties between each ACL bundle, the systematic connectivity of the menisci, and the tensile strength of each bundle. Therefore, this study aimed to characterize the morphological connectivity between the AM bundle and PL bundle of the ACL and the meniscus using nondestructive three-dimensional micro-CT and histological analyses. Quantitative analyses of histological characteristics of each bundle were also conducted. Our hypothesis was that differences in histological characteristics reflect the distinct biomechanical functions of the AM and PL bundles. Furthermore, it was expected that macroscopic and morphological alterations among bundles would be expected following ACL flexion. Such in-depth laboratory insight into the ACL bundle and meniscal connectivity would not only enhances our understanding of the mechanical causes of injury but also provides fundamental data for characterizing the ACL bundle in clinical ACL reconstruction.

Results

The AM and PL bundles of the ACL (Fig. 1A–D), as well as the meniscal roots to which each ACL is connected were thoroughly analyzed from multiple perspectives using MT, PC, saf-O, modified VG, and micro-CT (Fig. 2A–C).

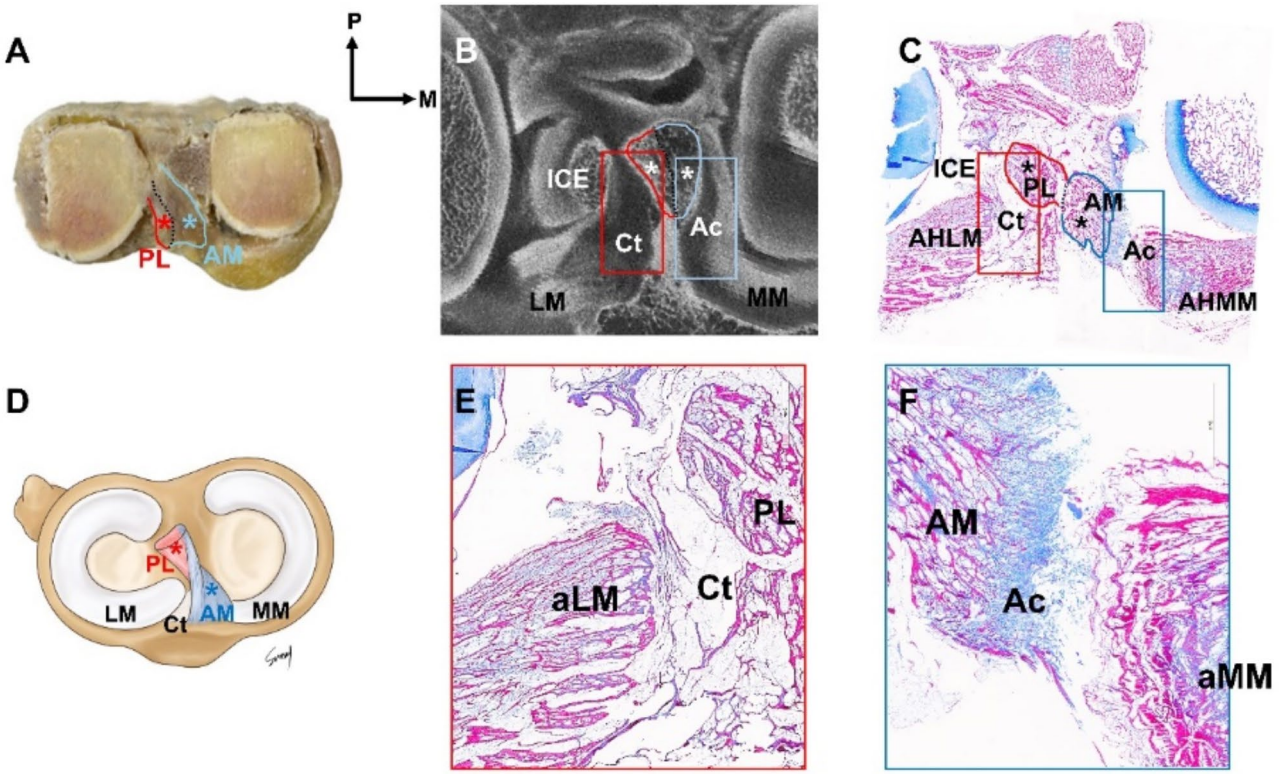

Fig. 1. The overall morphological transverse section of the knee joint complex (**A**–**F**). These structures were subsequently compared and analyzed using microcomputed tomography ((micro-CT, (**B**). Applying modified Masson's trichrome staining (MT) confirmed the connectivity of the anteromedial (AM) bundle of the anterior cruciate ligament (ACL) (C; blue asterisk), posterolateral (PL) bundle of the ACL (**C**); red asterisk)), and meniscus (**C**). The AM bundle tightly connected to the anterior horn of the medial meniscus (aMM) and articular cartilage (**F**); Ac, blue box)), while the PL bundle loosely connected to the anterior horn of the lateral meniscus (aLM) and connective tissue (**E**); Ct, red box)). *AM* anterior cruciate ligament-anteromedial bundle, *Ac* articular cartilage, *aLM* anterior horn of lateral meniscus, *aMM* anterior horn of medial meniscus, *Ct* connective tissue, *ICE* intercondylar eminence, *LM* lateral meniscus, *MM* medial meniscus, *PL* anterior cruciate ligament-posterolateral bundle.

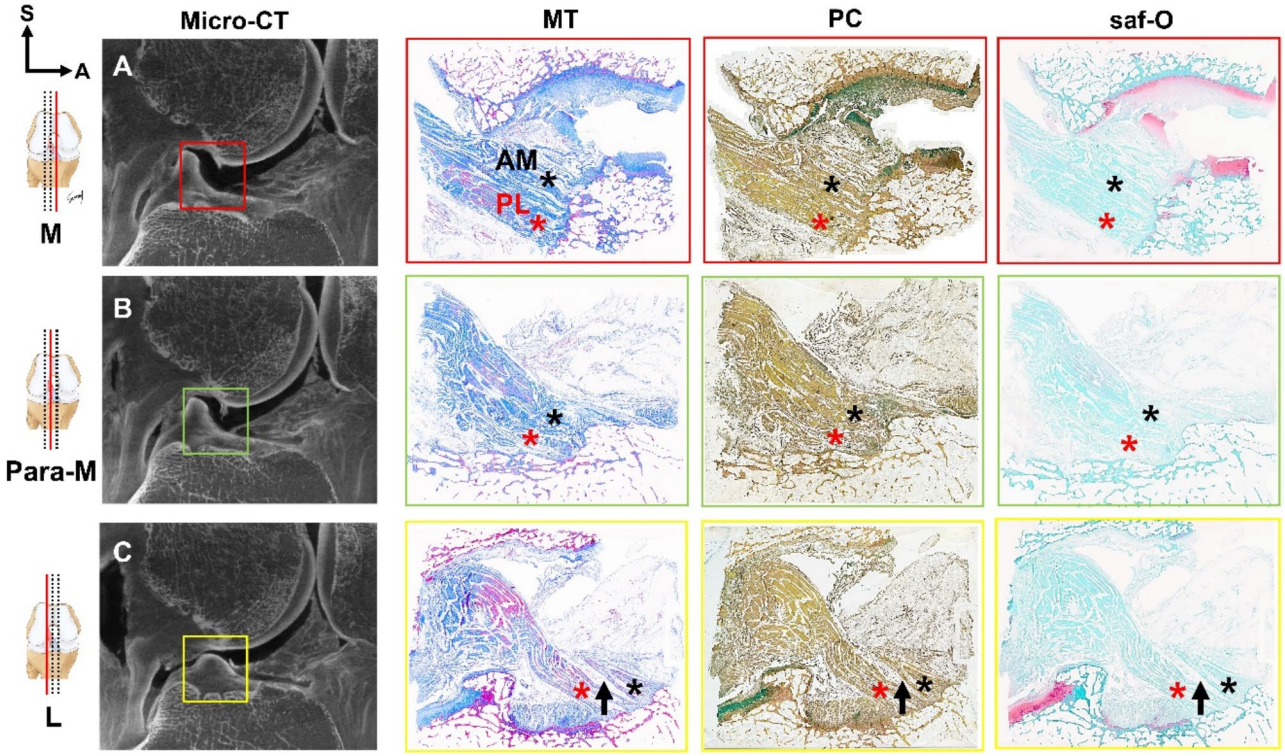

Fig. 2. Analysis of immunohistochemical staining (MT, PC, and saf-O) in serial sagittal sections of the knee joint flexed at 15° (**A**–**C**). Subsequently, the analysis results were compared using micro-CT. The space between the AM bundle (black asterisk) and the PL bundle (red asterisk) of the ACL was observed to gradually widened from the medial to the lateral side of the knee (indicated by the black arrow). This sequential arrangement of the ACL is illustrated from the red box to the yellow box (Supplemental Video 1). A: anterior, *L* lateral, *M* medial, *Micro-CT* micro-computed tomography, *MT* Masson's trichrome staining, *Para-M* para-medial, *PC* pentachrome staining, *saf-O safranin-O staining*, *S* superior.

Anatomical connectivity of the AM and PL bundles of the ACL

Cadaveric dissection (Fig. 1A), micro-CT (Fig. 1B) and histological observations (Fig. 1C–F) confirmed that the AM bundle of the ACL is densely connected to the medial meniscus by the articular cartilage (Fig. 1C, F). On the other hand, the PL bundle of the ACL is loosely attached to the transition zone of the lateral meniscus by the connective tissue (Fig. 1C, E).

Applying various histological staining techniques (MT, PC, and saf-O) revealed that in the sagittal view the region between the AM and PL bundles is bridged by connective tissue, and the interbundle space gradually widens from the medial to the lateral side (Fig. 2C and Supplemental Video 1).

The difference in knee flexion between 15 and 60° was analyzed using micro-CT and identified across various directions (Fig. 3A–F). Micro-CT examination of the coronal view (Fig. 3D), sagittal view (Fig. 3E), and horizontal view (Fig. 3F) at angles exceeding 60 degrees revealed divergences in the spaces occupied by the AM and PL bundles (Fig. 3D and F, and Supplemental Video 2).

Ratio of AM and PL bundles of the ACL

The histological characteristics of the AM and PL bundles were analyzed separately into upper and lower regions (Fig. 4A, B).

Among ACL fibers, the AM bundles exhibited a combination of wavy or twisted nonlinear networks, whereas the PL bundles appeared as parallel and regular patterns. Elastic fibers were found to run parallel between collagen bundles. Based on detailed histological findings, the proportions of collagen and elastic fibers were highest in the upper region of the AM bundle, at 84.68 ± 6.49 and 9.59 ± 0.60, respectively; Supplemental Fig. 1 A and 1B). Additionally, the ratio of elastic fibers to collagen was highest in this upper region (11.36 ± 0.90%, $p < 0.05$) and lowest in its lower region (4.87 ± 0.34%, $p < 0.05$) (Fig. 5A). The ratio of elastic to collagen fibers within the AM bundle of the ACL is indicative of functional differences in strength and flexibility. The upper AM, with a higher content of elastic fibers, demonstrates clinical responsiveness to movement and enhances flexibility. In contrast, the lower AM, which has a relatively higher collagen content, offers resistance to tensile strength when the upper AM is stretched.

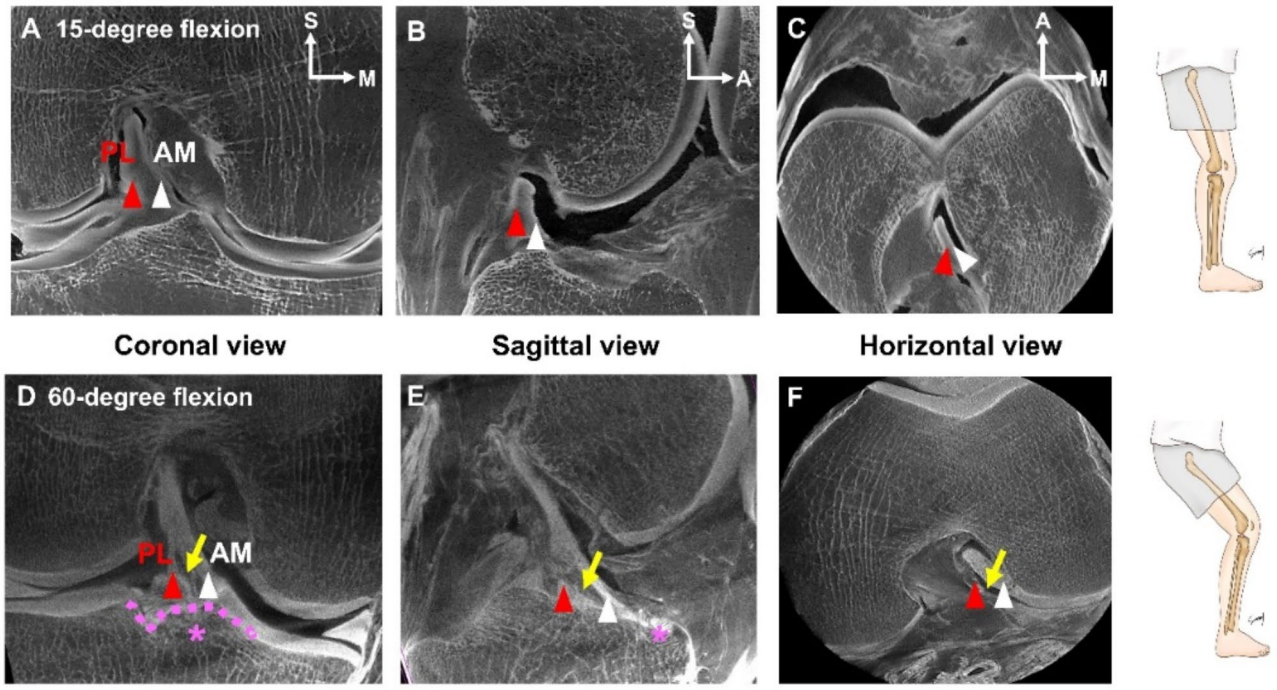

Fig. 3. Comparative analysis of 15° and 60° of knee flexion using micro-CT (**A**–**F**). The coronal view (**A**,**D**), sagittal view (**B**,**E**), and horizontal view (**C**,**F**) were analyzed for each angle to confirm morphological differences between the AM bundle (white arrowhead) and the PL bundle (red arrowhead) of the ACL. At 60 degrees of flexion, the gap between the AM bundle and the PL bundle gradually widened (Supplemental Video 2), becoming distinctly verified (indicated by the yellow arrow; **D**–**F**). The transverse ligament is denoted by the pink dotted line (pink asterisk; **D**,**E**). *A* anterior, *AM* anterior cruciate ligament-anteromedial bundle, *LM* lateral meniscus, *MM* medial meniscus, *M* medial, *P* posterior, *PL* anterior cruciate ligament-posterolateral bundle, *S* superior.

Quantitative measurements of upper region of ACL

In the upper region of the AM bundle, elastic fibers are abundant and predominantly clustered (9.59 ± 0.60%, $p < 0.05$), while the collagen fibers of the AM bundle of the ACL are also abundant, dense, and robust, but in a disorganized arrangement in various orientation (84.68 ± 6.49%, $p < 0.05$, Supplemental Fig. 1A). On the other hand, the collagen fiber in PL bundle of the ACL is in an organized arrangement but constitute a lower proportion that in the AM bundle (69.19 ± 5.55%, $p < 0.05$, Supplemental Fig. 1A). The elastic fibers exhibit sporadic, multidirectional patterns with a lower proportion (7.13 ± 0.32%, $p < 0.05$). The ratio of elastic fibers to collagen in the upper region was higher in the AM bundle than in the PL bundle (11.36 ± 0.90%, 10.33 ± 0.37%, respectively; Fig. 5A).

Quantitative measurements of lower region of ACL

The ratio of elastic fibers to collagen was lower for both the AM and PL bundles in the lower region than in the upper region of the ACL (4.87 ± 0.34% and 5.32 ± 0.78%, respectively; Fig. 5A). Additionally, the difference in the ratio of elastic fibers to collagen between the dense region (13.08%, Fig. 5B) and the loose region (4.70%) was found to be more pronounced for the PL bundle than the average lower regional ratio (5.32%). In the lower region of the AM bundle, the collagen proportion was 76.84 ± 7.50%, while the PL bundle had the lowest value of 63.08 ± 8.43% (see Supplemental Fig. 1A). Although the collagen content in the lower region was lower for the PL bundle than the AM bundle, the ratio of elastic fibers to collagen was higher in the PL bundle (5.32 ± 0.78%) than in the AM bundle (4.87 ± 0.34%, Fig. 5A). In summary, there appear to be notable differences in AM and PL bundle ratios in the upper and lower regions, which are confirmed by differences in the elastic fiber ratios related to collagen density.

Discussion

Understanding the biomechanical and clinical characterizes of the ACL requires a thorough knowledge of the microscopic properties of its two subparts - AM and PL bundles - which have not been studied in detail histologically. Herein, we have successfully demonstrated that the AM and PL bundles play essential kinetic roles in knee movement, acting as a primary fulcrum and an additional buffering cushion, respectively; (1) the AM bundle is composed of ligamentous segments with a denser, more-disorganized arrangement which are strongly connected to the medial meniscus. (2) the PL bundle is loosely attached to the lateral meniscus and contains ligamentous compartments with an organized arrangement. (3) during knee flexion, the length of the

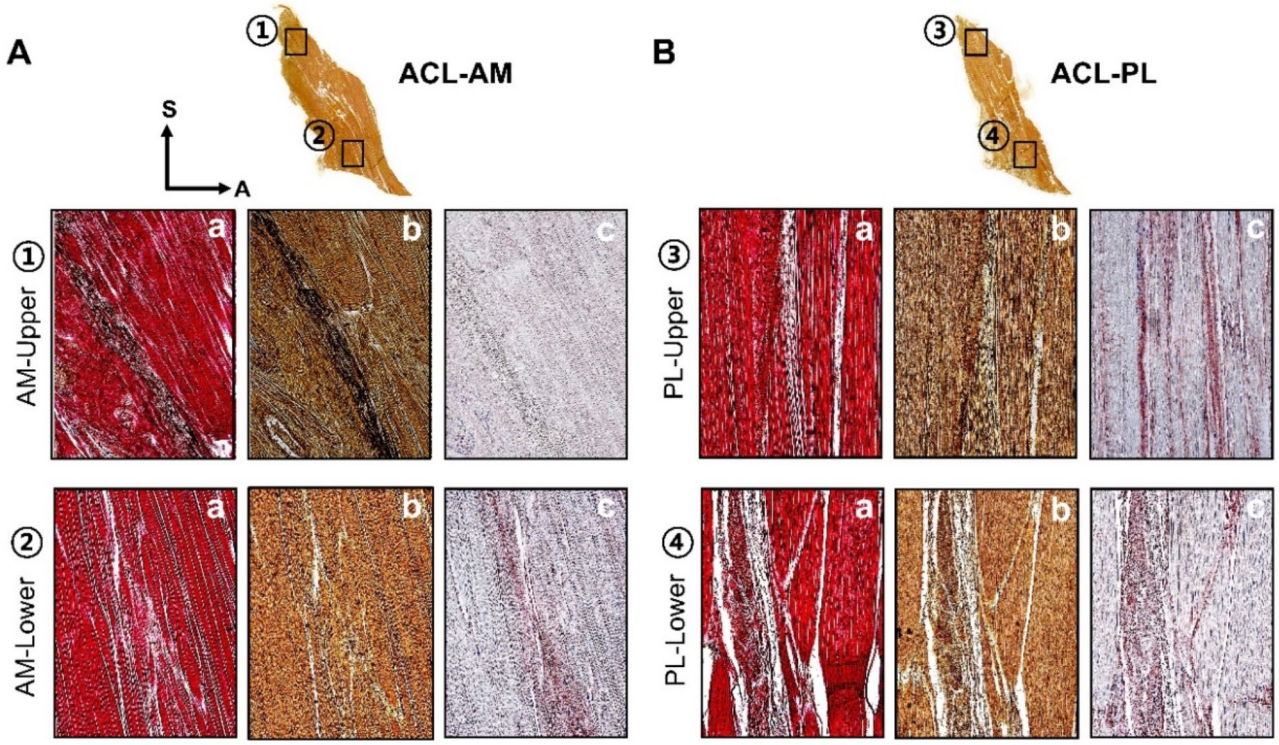

Fig. 4. Identification of histomorphological differences between the upper and lower regions of both the AM and PL bundles of the ACL using immunohistochemical methods (VG (a), PC (b), Collagen (c); (**A**,**B**). Modified Verhoeff–Van Gieson staining (a) confirmed the characteristics of collagen and elastic fibers in magnified images. Collagen is indicated in red, and black dots represent elastic fibers. In Pentachrome staining (b), elastic fibers appear as brownish collagen clusters with black dots and were further analyzed using collagen immunohistochemical staining. The upper region of the AM bundle (**A**) displays a dense concentration of elastic fibers, whereas the lower region exhibits a sporadic, multiskewed pattern. Similarly, in the PL bundle (**B**), the upper region contains more elastic fibers than in the lower region. The collagen arrangement in the AM bundle (A-c) appears to be densely disorganized, while in the PL bundle (B-c), it exhibits an organized pattern with a lower collagen proportion. *ACL-AM* anterior cruciate ligament-anteromedial bundle, *ACL-PL* anterior cruciate ligament-posterolateral bundle.

AM bundle extends more elastically with the medial meniscus remaining almost unchanged, whereas the PL bundle deviates laterally with a lower rigidity.

Fibrous blending of ACL and the lateral meniscus has been widely reported based on macroscopic and histological evidence[14–21]. In our study, two subparts of the ACL were histologically in contact with the adjacent meniscus on their ipsilateral side, not only the lateral but also the medial meniscus (Fig. 1A–F). The AM bundle directly overlapped the medial meniscus and articular cartilage of the medial tibial condyle, implying that its strong attachment to the medial meniscus maximizes joint stability during knee flexion[22]. Also, the direct connection of the AM bundle to the articular component suggests that responsive collagen production by chondrocytes in this junctional area can maintain the articular surface despite the constant mechanical stress to the knee joint[23]. Similar to other studies, the PL bundle was found to be inserted anteriorly to the anterior horn of the lateral meniscus[10,24]. The PL bundle is loosely connected to the lateral meniscus, with a transition zone of loose connective tissue forming the boundary between them.

The mechanical relationship between the subparts of the ACL and two menisci is important in distributing the axial load on the knee to ensure joint stability, and therefore meniscal tear are also strongly associated with ACL injuries[25]. Posterior displacement of the menisci during tibial rotation by knee flexion results in ACL retraction. The medial meniscus is more tightly attached to the bone, making it relatively less mobile than the lateral meniscus. In our study, the AM bundle may be a more solid fulcrum (Figs. 1 and 2). Namely, the AM bundle–medial meniscus–medial tibial condyle complex is stronger, more rigid, and more resistant than its counterpart[8]. In this 'medial' complex, injuries to the joints, ligaments, and meniscus are more commonly result mechanical damage or degenerative changes[26–29]. The fragile histological characteristics of the PL bundle and its connections to surrounding structures explain why the lateral meniscus is more susceptible to damage from ligament instability than from direct mechanical stress[21,30–32]. It corresponds that excessive stress on the knee joint would be concentrated on its lateral side, whereas it would be evenly distributed on the medial side, suggesting that the lateral meniscus is more susceptible to acute injury than the medial meniscus[33–36]. Arner et al.[37] also argued that ACL injury increases the likelihood of lateral meniscus displacement, alters the contact

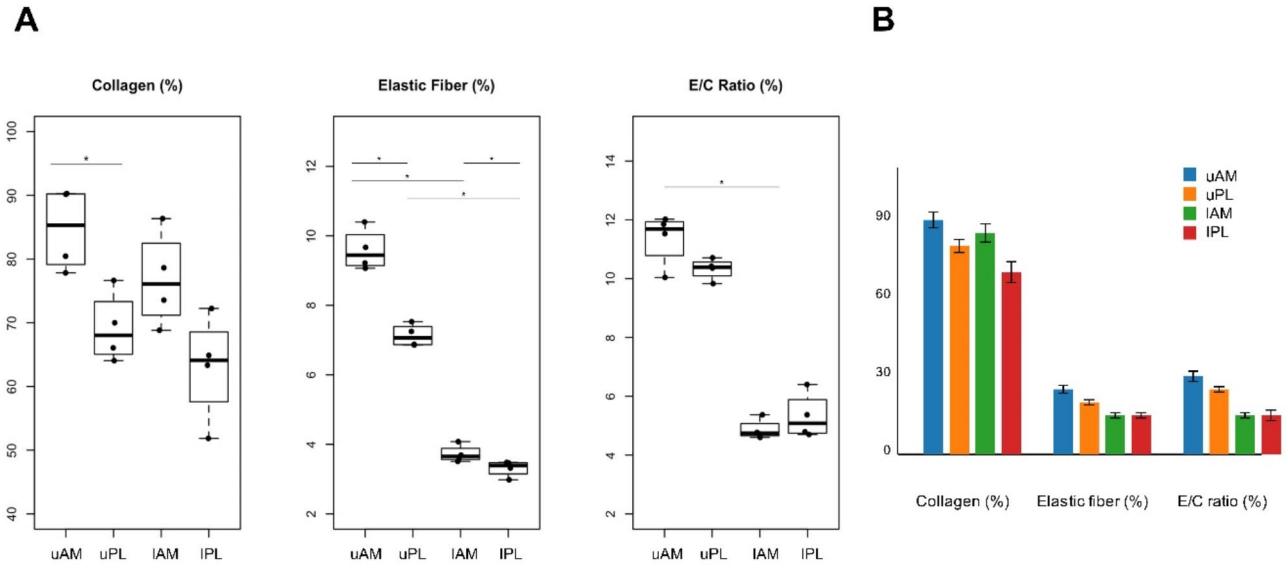

Fig. 5. Graphs depicting the area ratio of elastic fibers to collagen in four regions of the ACL based on Fig. 4. The ratio for the AM bundle was highest in the upper regions, at 11.36 ± 0.90% ($p < 0.05$), and lowest in the lower region, at 4.87 ± 0.34% ($p < 0.05$), (**A**). Analysis of the regional composition of the PL bundle revealed that the dense area accounted for 10.33 ± 0.37% and the loose area accounted for 5.32 ± 0.78% ($p < 0.05$), (**A**). As demonstrated in Figure (**B**), the figures for each area were presented through the master chart. The boxplots display regional differences in the E/C ratio (elastic fiber/collagen fiber area ratio), with each box indicating median, 25th and 75th percentiles, and range values. Statistical significance ($p < 0.05$) is indicated by asterisks. E/C ratio, elastic fiber/collagen fiber area ratio; lAM, lower anteromedial bundle; lPL, lower posterolateral bundle; uAM, upper anteromedial bundle; uPL, upper posterolateral bundle.

position of the articular cartilage, and elevates chronic tension in the medial meniscus. In other words, our finding implies that temporary acute displacement due to injury is more common in the PL bundle, whereas sustained extrinsic forces causing injurious compression are more common in the AM bundle (Figs. 1 and 1).

At 60 and 90 degrees of knee flexion, tibial anterior shear force increases, placing greater stress on the ACL. Our findings suggest that the two bundles diverge laterally from the medial side of the knee due to the stretching of the connective tissue that occurs during knee flexion (Fig. 3 and Supplemental Video 2). The meniscus contributes to widening the space between these bundles and the likelihood of injury increases when the knee is flexed beyond 60 degrees. Stress in front of the ACL is localized at the anterior site of the intercondylar fossa, altering the orientation of the ligament. The transverse ligament, anchored to the front of bilateral menisci, is critical for knee rotation and restricts early flexion of the medial meniscus, thereby influencing ACL alignment. Up to 60 degrees of flexion, the position of the menisci remains stable, but flexion beyond this point can lead to meniscal damage. Extreme torque can lead to the unfortunate triad syndrome in which injuries to the ACL and adjacent structures occur simultaneously.

Differences between the bundles in collagen density and mechanical behavior have implications for shear force capacity and flexibility, as they may indicate injury susceptibility and kinematic differences within the ACL. In our study, the AM and PL bundles differ in collagen density and mechanical behavior, which affects shear force capacity and flexibility, and may indicate injury susceptibility and kinematic differences within the ACL (Figs. 4 and 5). The eccentric tensile strength of the AM bundle exceeds that of the PL bundle at knee flexions greater than 60 degrees. Previous arthroscopic studies have associated ACL hypermobility and damage to the anterior horn of the medial meniscus with anterior knee pain and an increased risk of meniscal tears[38]. The tensile force is higher in the AM bundle attached to the anterior horn of the medial meniscus than in the PL bundle attached to the lateral meniscus, which is due to the difference in size of the attachment sites on the horn[39]. The stiffness of these sites and the different tissue characteristics may play a role in the mechanism of injury.

The study faced several challenges: (1) The sample size was small, yet we established data significance and used a combination of macroscopic histology and 3D micro-CT to compensate for the sample number. (2) Our focus was on the histology and proportions of the AM and PL bundles, not including the kinematic analysis of translation and torsion relating to the transverse ligament. (3) The age of the cadaver specimens might have affected the outcomes, as collagen content and tensile strength decrease with age[40,41]. Hence, more comprehensive biomechanical studies on torque values are recommended for future research.

Materials and methods

Specimen preparation

This descriptive cadaveric study was conducted in the translatory laboratory for clinical anatomy at our medical research facility. Ten unembalmed human cadavers (5 males and 5 females; 15 sides) with an age at death of 69.1 ± 8.3 years (mean ± standard deviation) were included. Body donors had previously provided an informed

consent statement to participate in the body donation program of Surgical Anatomy Education Centre at Yonsei University College of Medicine. Ethical approval for this study was obtained from the Institutional Review Board of Yonsei University College of Medicine (Yonsei IRB Approval number: 4-2023-0823). This study was conducted in accordance with the principles of the Declaration of Helsinki.

Manual dissection

The specimens were dissected while taking particular care to remove all soft tissues surrounding the knee joint, with special attention given to preserving the two bundles of the ACL. Cadavers with a history of traumatic events, clinically visible deformities, meniscal tears, or arthroscopic partial meniscectomy around the knee were excluded. An anatomical saw was used for dissection in order to prevent damage to the ACL and neighboring tissues, except for the ACL, meniscus, collateral ligaments, surrounding soft tissues, and vessels. The medial parapatellar incision was performed meticulously, the patella was flipped over, and the ACL at the bone–ligamentous junction of the femur and tibia was incised and harvested. The surrounding fibrous membrane and fatty tissue were methodically excised and separated along the marginal border between the AM and PL bundles of the ACL.

Histology

Tissue blocks were decalcified and embedded in paraffin wax, followed by serial sectioning into 5-μm-thick slices. The histological analysis was performed using modified Masson's trichrome staining (MT), Pentachrome staining (PC), and Safranin-O staining (saf-O), modified Verhoeff–Van Gieson staining (VG) techniques.

Modified Masson's trichrome staining

Specimens were incubated in a decalcification solution for 3 days and neutralized by soaking in a 0.25% lithium-carbonate solution for 4 h. After embedding in paraffin, 5-μm thick sections were obtained. Deparaffinization and rehydration were performed, followed by preservation in Bouin's solution at 60 ℃ for 1 h. Weigert's iron hematoxylin and Biebrich scarlet/acid fuchsin solutions were used, and differentiation was achieved in a 2.5% phosphomolybdic acid–phosphotungstic acid solution. Aniline blue solution was applied, followed by 1% acetic acid solution.

Pentachrome staining

After dehydration, the elastic fibers were stained using Verhoeff's iron hematoxylin stain, followed by staining of glycosaminoglycan (GAG) with Alcian blue (pH 2.5) solution. The muscles were subsequently stained with Biebrich scarlet–acid fuchsin solution and differentiated with 5% phosphotungstic acid solution. Finally, collagen was stained with a yellow solution. Through this process, PC staining intricately delineates the tissue architecture by displaying the collagen, elastic fibers, muscle fibers, fibrin, and GAG in distinct colors.

Safranin-O staining

To stain the nuclei, 5 μm-thick tissue sections were immersed in Weigert's iron hematoxylin solution for 10 min. Subsequently, a 0.001% solution of Fast Green (FCF) was applied for 5 min, followed by 1% Acetic acid solution and 0.1% saf-O solution for 5 min each. This process results in the cartilage matrix is being stained red while the surrounding background appears green.

Modified verhoeff–Van Gieson staining

Sections underwent a deparaffinization process using xylene, followed by sequential rehydration in 100%, 95%, and 70% ethanol solutions for 1 min each. After a 5-minute immersion in distilled water, the sections were incubated in a working Elastic Stain Solution (Abcam, Cambridge, United Kingdom) for 30 min and subsequently washed in running tap water. Differentiation was achieved using 2% ferric chloride, followed by treatment with 5% sodium thiosulfate for 1 min. The sections were then incubated in modified VG solution for 3 min, dehydrated in ethanol, and cleared with xylene. Following staining, the samples underwent further ethanol dehydration and were cleared in xylene.

Analysis of the AM and PL bundle of the ACL

An optical microscope (BX51, Olympus, Tokyo, Japan) were used to examine all sections. Using ImageJ software (Java 1.8.0, National Institutes of Health, Bethesda, MD, United States) was used to measure the two-dimensional area of signals indicating the presence of collagen type I and elastic fibers at identical positions. The densities of collagen and elastic fibers were compared and analyzed by delineating the upper and lower regions of the AM and PL bundles of the ACL. The ratio of elastic fibers to collagen was calculated relative to the cross-sectional area.

The statistical significance of the ratio of elastic fibers to collagen was standardized using R software (version 4.2.2 in a MS Windows). Morphometric data are presented as a mean ± standard deviation. A paired *t*-test was utilized due to the normal distribution of the data, with a p-value < 0.05 considered significant.

PTA preparation and micro-CT analysis

The knee joints used in the study was kept intact, without any removal of skin or fat, and free from degenerative soft tissue changes. In order to ensure that the two bundles of the ACL and meniscus could be clearly visualized, the intercondylar portion of the femur was carefully sectioned while preserving the attachment sites. It has been reported that the micro-CT preparation technique can increase the contrast enhancement of soft tissues[42].

The knee specimens from the seven cadavers were subjected to a sequential immersion process in 30%, 50%, and 70% ethanol solutions overnight, which was followed by a 2% PTA solution with 70% ethanol for a period of

1 month. The specimens were then scanned using a micro-CT scanner (Skyscan1173, Bruker, Kontich, Belgium) with the following conditions: source voltage of 110 kV, source current of 72 μA, image pixel grid of 940 × 759; and image pixel size of 72 inches. For 3D visualization and analysis, all scanned images were reconstructed using NRecon and CTVox software (version 2.7 software, Bruker, Kontich, Belgium) and analyzed using Mimics software (version 20.0 software, Materialise, Leuven, Belgium).

Data availability

The datasets analyzed during the current study are available from the corresponding author on reasonable request.

Received: 30 July 2024; Accepted: 23 January 2025
Published online: 25 February 2025

References

1. Sullivan, D., Levy, I. M., Sheskier, S., Torzilli, P. A. & Warren, R. F. Medial restraints to anterior-posterior motion of the knee. *J. Bone Joint Surg. Am.* **66**, 930–936. https://doi.org/10.2106/00004623-198466060-00015 (1984).
2. Fu, F., Shen, H., Starman, W., Okeke, J. S., Irrgang, J. J. & N., & Primary anatomic double-bundle Anterior Cruciate Ligament Reconstruction: a preliminary 2-Year prospective study. *Am. J. Sports Med.* **36**, 1263–1274. https://doi.org/10.1177/0363546508314428 (2008).
3. Jerosch, J., Prymka, M. & Castro, W. H. Proprioception of knee joints with a lesion of the medial meniscus. *Acta Orthop. Belg.* **62**, 41–45 (1996).
4. Smith, J. P. I. I. I. & Barrett, G. R. Medial and lateral meniscal tear patterns in anterior cruciate ligament-deficient knees: a prospective analysis of 575 tears. *Am. J. Sports Med.* **29**, 415–419. https://doi.org/10.1177/03635465010290040501 (2001).
5. Wyatt, R., Inacio, W., Liddle, M. C., Maletis, G. B. & K. D., & Factors associated with meniscus repair in patients undergoing anterior cruciate ligament reconstruction. *Am. J. Sports Med.* **41**, 2766–2771. https://doi.org/10.1177/0363546513503287 (2013).
6. Arnoczky, S. P. Anatomy of the anterior cruciate ligament. *Clin. Orthop. Relat. Res.* **172**, 19–25 (1983).
7. Girgis, F., Marshall, G., Monajem, A. & J, L., & The cruciate ligaments of the knee joint. Anatomical, functional and experimental analysis. *Clin. Orthop. Relat. Res.* **106**, 216–231. https://doi.org/10.1097/00003086-197501000-00033 (1975).
8. Norwood, L. A. & Cross, M. J. Anterior cruciate ligament: functional anatomy of its bundles in rotatory instabilities. *Am. J. Sports Med.* **7**, 23–26. https://doi.org/10.1177/036354657900700106 (1979).
9. Nikolic, D. K. Lateral meniscal tears and their evolution in acute injuries of the anterior cruciate ligament of the knee. Arthroscopic analysis. *Knee Surg. Sports Traumatol. Arthrosc.* **6**, 26–30. https://doi.org/10.1007/s001670050068 (1998).
10. LaPrade, C. M. et al. Anatomy of the anterior root attachments of the medial and lateral menisci: a quantitative analysis. *Am. J. Sports Med.* **42**, 2386–2392. https://doi.org/10.1177/0363546514544678 (2014).
11. LaPrade, C. M. et al. Consequences of tibial tunnel reaming on the meniscal roots during cruciate ligament reconstruction in a cadaveric model, part 1: the anterior cruciate ligament. *Am. J. Sports Med.* **43**, 200–206. https://doi.org/10.1177/0363546514554769 (2015).
12. Staübli, H. U. & Rauschning, W. Tibial attachment area of the anterior cruciate ligament in the extended knee position. Anatomy and cryosections in vitro complemented by magnetic resonance arthrography in vivo. *Knee Surg. Sports Traumatol. Arthrosc.* **2**, 138–146. https://doi.org/10.1007/BF01467915 (1994).
13. Santiago, F., García, R., Fernández, M. D. M. C., Sánchez, J. T. & J. M. T., & Anomalous insertion of anterior cruciate ligament band into the transverse ligament. *Eur. J. Radiol.* **68**, 33–35. https://doi.org/10.1016/j.ejrex.2008.06.001 (2008).
14. Fujishiro, H. et al. Attachment area of fibres from the horns of lateral meniscus: anatomic study with special reference to the positional relationship of anterior cruciate ligament. *Knee Surg. Sports Traumatol. Arthrosc.* **25**, 368–373. https://doi.org/10.1007/s00167-015-3813-3 (2017).
15. Kusano, M. et al. Tibial insertions of the anterior cruciate ligament and the anterior horn of the lateral meniscus: a histological and computed tomographic study. *Knee* **24**, 782–791. https://doi.org/10.1016/j.knee.2017.04.014 (2017).
16. Purnell, M. L., Larson, A. I. & Clancy, W. Anterior cruciate ligament insertions on the tibia and femur and their relationships to critical bony landmarks using high resolution volume-rendering computed tomography. *Am. J. Sports Med.* **36**, 2083–2090. https://doi.org/10.1177/0363546508319896 (2008).
17. Siebold, R., Ellert, T., Metz, S. & Metz, J. Tibial insertions of the anteromedial and posterolateral bundles of the anterior cruciate ligament: morphometry, arthroscopic landmarks, and orientation model for bone tunnel placement. *Arthroscopy* **24**, 154–161. https://doi.org/10.1016/j.arthro.2007.08.006 (2008).
18. Siebold, R. et al. Flat midsubstance of the anterior cruciate ligament with tibial C-shaped insertion site. *Knee Surg. Sports Traumatol. Arthrosc.* **23**, 3136–3142 (2015).
19. Zantop, T., Wellmann, M., Fu, F. H. & Petersen, W. Tunnel positioning of anteromedial and posterolateral bundles in anatomic anterior cruciate ligament reconstruction. *Am. J. Sports Med.* **36**, 65–72. https://doi.org/10.1177/0363546507308361 (2008).
20. Tensho, K. et al. Bony landmarks of the anterior cruciate ligament tibial footprint: a detailed analysis com paring 3-dimensional computed tomography images to visual and histological evaluations. *Am. J. Sports Med.* **42**, 1433–1440. https://doi.org/10.1177/0363546514528789 (2014).
21. Ferretti, A., Monaco, E., Fabbri, M., Maestri, B. & De Carli, A. Prevalence and Classification of Injuries of Anterolateral Complex in Acute Anterior Cruciate ligament tears. *Arthroscopy* **33**, 147–154. https://doi.org/10.1016/j.arthro.2016.05.010 (2017).
22. Petersen, W. & Tillmann, B. Structure and vascularisation of the cruciate ligaments of the human knee joint. *Anat. Embryol.* **200**, 325–334. https://doi.org/10.1007/s004290050283 (1999).
23. Akkiraju, H. & Nohe, A. Role of chondrocytes in cartilage formation, progression of osteoarthritis and cartilage regeneration. *J. Dev. Biol.* **3**, 177–192. https://doi.org/10.3390/jdb3040177 (2015).
24. Johnson, D. L. et al. Insertion-site anatomy of the human menisci: gross, arthroscopic, and topographical anatomy as a basis for meniscal transplantation. *Arthroscopy* **11**, 386–394. https://doi.org/10.1016/0749-8063(95)90188-4 (1995).
25. Baker, B. E., Peckham, A. C., Pupparo, F. & Sanborn, J. C. Review of meniscal injury and associated sports. *Am. J. Sports Med.* **13**, 1–4. https://doi.org/10.1177/036354658501300101 (1985).
26. Andriacchi, T. P., Briant, P. L., Bevill, S. L. & Koo, S. Rotational changes at the knee after ACL injury cause cartilage thinning. *Clin. Orthop. Relat. Res.* **442**, 39–44. https://doi.org/10.1097/01.blo.0000197079.26600.09 (2006).
27. Shefelbine, S. J. et al. MRI analysis of in vivo meniscal and tibiofemoral kinematics in ACL-deficient and normal knees. *J. Orthop. Res.* **24**, 1208–1217. https://doi.org/10.1002/jor.20139 (2006).
28. Abebe, E. S. et al. The effects of femoral graft placement on in vivo knee kinematics after anterior cruciate ligament reconstruction. *J. Biomech.* **44**, 924–929. https://doi.org/10.1016/j.jbiomech.2010.11.028 (2011).
29. Karpinski, K., Forkel, P., Häner, M., Bierke, S. & Petersen, W. Etiology of posterior meniscus root tears: medial vs. lateral. *Arch. Orthop. Trauma. Surg.* **143**, 429–437. https://doi.org/10.1007/s00402-022-04347-y (2023).

30. Thompson, W. O., Thaete, F. L., Fu, F. H. & Dye, S. F. Tibia1 meniscal dynamics using three-dimensional reconstruction of magnetic resonance images. *Am. J. Sports Med.* **19**, 210–216. https://doi.org/10.1177/036354659101900302 (1991).
31. Bylski-Austrow, D. I., Ciarelli, M. J., Kayner, D. C., Matthews, L. S. & Goldstein, S. A. Displacements of the menisci under joint load an in vitro study in human knees. *J. Biomech.* **27**, 421–431. https://doi.org/10.1016/0021-9290(94)90018-3 (1994).
32. Mehl, J. et al. The ACL-deficient knee and the prevalence of meniscus and cartilage lesions: a systematic review and meta-analysis (CRD42017076897). *Arch. Orthop. Trauma. Surg.* **139**, 819–841. https://doi.org/10.1007/s00402-019-03128-4 (2019).
33. Walker, P. S. & Erkiuan, M. J. The role of the menisci in force transmission across the knee. *Clin. Orthop. Relat. Res.* **109**, 184–192. https://doi.org/10.1097/00003086-197506000-00027 (1975).
34. Bhatia, S., LaPrade, C. M., Ellman, M. B. & LaPrade, R. F. Meniscal root tears: significance, diagnosis, and treatment. *Am. J. Sports Med.* **42**, 3016–3030. https://doi.org/10.1177/0363546514524162 (2014).
35. Feucht, M. J. et al. Associated tears of the lateral meniscus in anterior cruciate ligament injuries: risk factors for different tear patterns. *J. Orthop. Surg. Res.* **10**, 1–8. https://doi.org/10.1186/s13018-015-0184-x (2015).
36. Forkel, P. et al. Different patterns of lateral meniscus root tears in ACL injuries: application of a differentiated classification system. *Knee Surg. Sports Traumatol. Arthrosc.* **23**, 112–118. https://doi.org/10.1007/s00167-014-3467-6 (2015).
37. Arner, J. W. et al. The effects of anterior cruciate ligament deficiency on the meniscus and articular cartilage: a novel dynamic in vitro pilot study. *Orthop. J. Sports Med.* **4**, 2325967116639895. https://doi.org/10.1177/2325967116639895 (2016).
38. Shiwaku, K. et al. The role of the medial meniscus in anterior knee stability. *Orthop. J. Sports Med.* **10**, 23259671221132845. https://doi.org/10.1177/23259671221132845 (2022).
39. Ellman, M. B. et al. Return to play following anterior cruciate ligament reconstruction. *J. Am. Acad. Orthop. Surg.* **23**, 283–296. https://doi.org/10.5435/JAAOS-D-13-00183 (2015).
40. Woo, S. L., Hollis, J. M., Adams, D. J., Lyon, R. M. & Takai, S. Tensile properties of the human femur-anterior cruciate ligament-tibia complex: the effects of specimen age and orientation. *Am. J. Sports Med.* **19**, 217–225. https://doi.org/10.1177/036354659101900303 (1991).
41. Shin, J. W. et al. Molecular mechanisms of dermal aging and antiaging approaches. *Int. J. Mol. Sci.* **20**, 2126. https://doi.org/10.3390/ijms20092126 (2019).
42. Jehoon, O., Kwon, H. J., Kim, S. H., Cho, T. H. & Yang, H. M. Use of micro X-ray computed tomography with phosphotungstic acid preparation to visualize human fibromuscular tissue. *JoVE* **5**, 151e59752. https://doi.org/10.3791/59752 (2019).

Acknowledgements

The authors sincerely thank those who donated their bodies to science for anatomical research. The results of such research support the advancement of medical knowledge, which can improve patient care. Therefore, the donors and their families deserve the highest gratitude. All author also special thank Seonui Choi for providing the figure material.

Author contributions

I-S.Y: Formal analysis, Investigation, Data curation, Software, Visualization, Writing – original draft. J-E.H: Visualization, Methodology.H-M.Y: Conceptualization, Data curation, Formal analysis, Funding acquisition, Investigation, Methodology, Project administration, Resources, Writing – review and editing.All authors read and provided final approval of the version to be published.

Funding

This work was supported by the National Research Foundation Korea grant funded by the Korean government (No. RS-2023-00246638) and a grant of the Korea Health Technology R&D Project through the Korea Health Industry Development Institute (KHIDI), funded by the Ministry of Health & Welfare, Republic of Korea (grant number: RS-2024-00406488).

Declarations

Competing interests

The authors declare no competing interests.

Additional information

Supplementary Information The online version contains supplementary material available at https://doi.org/10.1038/s41598-025-88037-w.

Correspondence and requests for materials should be addressed to H.-M.Y.